

## IMMUNOBIOLOGY

# Virus-associated activation of innate immunity induces rapid disruption of Peyer's patches in mice

Simon Heidegger,<sup>1</sup> David Anz,<sup>1</sup> Nicolas Stephan,<sup>1</sup> Bernadette Bohn,<sup>1</sup> Tina Herbst,<sup>2</sup> Wolfgang Peter Fendler,<sup>1</sup> Nina Suhartha,<sup>1,2</sup> Nadja Sandholzer,<sup>1</sup> Sebastian Kobold,<sup>1</sup> Christian Hotz,<sup>1,2</sup> Katharina Eisenächer,<sup>3</sup> Susanne Radtke-Schuller,<sup>4</sup> Stefan Endres,<sup>1</sup> and Carole Bourquin<sup>1,2</sup>

<sup>1</sup>Center for Integrated Protein Science Munich, Division of Clinical Pharmacology, Medizinische Klinik und Poliklinik IV, Ludwig-Maximilians-Universität München, Munich, Germany; <sup>2</sup>Chair of Pharmacology, Department of Medicine, Faculty of Science, University of Fribourg, Fribourg, Switzerland; <sup>3</sup>II. Medizinische Klinik, Klinikum Rechts der Isar, Technische Universität München, Munich, Germany; and <sup>4</sup>Department of Biology II, Ludwig-Maximilians-Universität München, Planegg-Martinsried, Germany

## Key Points

- Systemic virus infection leads to rapid disruption of the Peyer's patches but not of peripheral lymph nodes.
- Virus-associated innate immune activation and type I IFN release blocks trafficking of B cells to Peyer's patches.

Early in the course of infection, detection of pathogen-associated molecular patterns by innate immune receptors can shape the subsequent adaptive immune response. Here we investigate the influence of virus-associated innate immune activation on lymphocyte distribution in secondary lymphoid organs. We show for the first time that virus infection of mice induces rapid disruption of the Peyer's patches but not of other secondary lymphoid organs. The observed effect was not dependent on an active infectious process, but due to innate immune activation and could be mimicked by virus-associated molecular patterns such as the synthetic double-stranded RNA poly(I:C). Profound histomorphologic changes in Peyer's patches were associated with depletion of organ cellularity, most prominent among the B-cell subset. We demonstrate that the disruption is entirely dependent on type I interferon (IFN). At the cellular level, we show that virus-associated immune activation by IFN- $\alpha$  blocks B-cell trafficking to the Peyer's patches by

downregulating expression of the homing molecule  $\alpha_4\beta_7$ -integrin. In summary, our data identify a mechanism that results in type I IFN-dependent rapid but reversible disruption of intestinal lymphoid organs during systemic viral immune activation. We propose that such rerouted lymphocyte trafficking may impact the development of B-cell immunity to systemic viral pathogens. (*Blood*. 2013; 122(15):2591-2599)

## Introduction

The innate immune system represents the first line of defense against invading viruses. The initiation of an antiviral response is critically dependent on the detection of specific pathogen-associated molecular patterns by innate immune pattern-recognition receptors.<sup>1</sup> These patterns are evolutionarily highly conserved molecular structures shared by a variety of different viruses. One such pattern is viral RNA, which can be detected by members of the retinoic acid inducible gene I-like receptor and Toll-like receptor families.<sup>2,3</sup> Activation of these receptors leads to the initiation of an innate immune response characterized by the rapid production of proinflammatory cytokines such as the type I interferons (IFNs) IFN- $\alpha$  and IFN- $\beta$ . At the infected site, type I IFNs act in concert with other cytokines to hinder the replication and spread of virus and to recruit inflammatory cells. In addition, these cytokines have systemic effects that can critically shape the subsequent adaptive immune response.<sup>4</sup>

Adaptive immunity depends on lymphocyte maturation in primary lymphoid organs, their tightly regulated release into the circulation, and accurate positioning in secondary lymphoid organs. Several reports have recently highlighted the impact of virus-associated type I IFNs on lymphocyte development and distribution: In bone marrow,

dormant hematopoietic stem cells that give rise to virtually all leukocytes have been shown to enter the cell cycle after intravenous injection of type I IFNs and during virus infection.<sup>5</sup> We and others have demonstrated that activation of virus-sensing innate immune receptors with the synthetic double-stranded RNA poly(I:C) leads to type I IFN-dependent rapid involution of the thymus.<sup>6</sup> In skin-draining peripheral lymph nodes (PLNs), poly(I:C)-induced type I IFNs have been shown to block lymphocyte egress, which results in temporary lymphoid organ "shutdown."<sup>7</sup> However, little is known about the influence of virus infection on lymphocyte distribution in secondary lymphoid organs of the intestinal immune compartment.

Many viruses, including those classically considered nonenteric, frequently show intestinal involvement due to either direct infection of the gut mucosa or collateral effects.<sup>8</sup> In the course of such an enteric infection, aggregated lymphoid follicles in the gut wall (ie, the Peyer's patches) form the primary inductive site of intestinal antimicrobial immunity.<sup>9,10</sup> In this study, we investigated the effect of virus-associated innate immune activation on lymphocyte distribution within these organs. Here we show for the first time that viral immune activation substantially changes the morphology of the

Submitted January 31, 2013; accepted June 26, 2013. Prepublished online as *Blood* First Edition paper, July 3, 2013; DOI 10.1182/blood-2013-01-479311.

S.H. and D.A. contributed equally to this study.

The online version of this article contains a data supplement.

The publication costs of this article were defrayed in part by page charge payment. Therefore, and solely to indicate this fact, this article is hereby marked "advertisement" in accordance with 18 USC section 1734.

© 2013 by The American Society of Hematology

Peyer's patches by inducing their rapid disruption. A marked type I IFN-dependent loss of cellularity was associated with strongly reduced B-cell trafficking to the Peyer's patches. Our data identify a mechanism that results in rapid but reversible loss of B cells in Peyer's patches during virus-associated systemic innate immune activation. We hypothesize that such rerouting of lymphocyte trafficking during systemic infection may be important for effective antiviral B-cell immunity.

## Methods

### Mice

Female C57BL/6 mice were purchased from Harlan-Winkelmann and Janvier. Type I IFN receptor-deficient mice (IFNAR<sup>-/-</sup>) were backcrossed 20 times on the C57BL/6 background.<sup>11</sup> Mice were at least 8 weeks of age at the onset of experiments. All animal studies were approved by the local regulatory agencies (Regierung von Oberbayern, Munich, Germany, and Etat de Fribourg, Fribourg, Switzerland).

### Injection of poly(I:C), recombinant IFN- $\alpha$ , virus, and blocking antibody

Mice were injected intraperitoneally with poly(I:C) (InvivoGen) (250  $\mu$ g in phosphate-buffered saline [PBS]). For examination of lymphoid organ cellularity, mice were treated twice at a 3-day interval. In all other experiments, mice were treated with a single injection of poly(I:C). Where indicated, mice were provided with drinking water supplemented with FTY720 (Sigma-Aldrich; 2  $\mu$ g/mL) beginning 2 days prior to the first poly(I:C) treatment. IFN- $\alpha$  (Miltenyi) was applied intraperitoneally (12  $\mu$ g in 200  $\mu$ L PBS) daily on 6 consecutive days. Twenty-four hours after the last injection, lymphoid organs were examined. For viral infection, mice were intraperitoneally injected with 10<sup>6</sup> plaque-forming units of vesicular stomatitis virus (VSV) *Indiana strain* in 200  $\mu$ L PBS. Lymphoid organs were examined 2 or 5 days after virus injection. For in vivo  $\alpha_4\beta_7$  blockade, mice were injected intraperitoneally with 75  $\mu$ g anti- $\alpha_4\beta_7$  antibody (clone DATK32) or a rat isotype control antibody (AbD Serotec, Puchheim, Germany) in 100  $\mu$ L PBS. Purification of DATK32 antibody from the DATK32 hybridoma cell line (ATCC, Manassas, VA) is described in detail in the supplemental Materials and methods (see the *Blood* Web site).

### Tissue preparation

Tissue single-cell suspensions were prepared as described previously.<sup>12</sup> For the determination of lymphocyte numbers in secondary lymphoid organs, bilateral inguinal and axillary lymph nodes were pooled (PLNs). For mesenteric lymph nodes, all lymph nodes along the full length of the superior mesenteric artery to the aortic root were dissected as described.<sup>13</sup> All Peyer's patches were prepared and were pooled for further analysis. Isolation of lymphocytes from small intestine lamina propria was performed as described previously.<sup>14</sup> Briefly, small intestine was removed 0.5 cm below the stomach and 1 cm above the cecum. Peyer's patches were removed surgically. The intestine was opened longitudinally and cut into pieces of 0.5 to 1 cm in length. Epithelial cells and intraepithelial lymphocytes were detached by several washing steps with Hanks' balanced salt solution containing 1 mM dithiothreitol or 1.3 mM EDTA. Pieces of small intestine were then enzymatically digested with the help of collagenase VIII (Sigma-Aldrich). Single-cell suspensions were purified using 44% to 67% Percoll (Sigma-Aldrich) gradient centrifugation.

### Flow cytometry

Antibodies to CD3 (Clone: 17A2), CD4 (RM4-5), CD8 (53-6.7), CD11c (N418), CD19 (6D5), CD69 (H1.2F3),  $\alpha_4\beta_7$  (DATK32), and CD62L (MEL-14) were purchased from BioLegend. Antibodies to Foxp3 (FJK-16a) and sphingosine-1 phosphate receptor 1 (S1P<sub>1</sub>) (713412) were from eBioscience and R&D Systems. Cells were stained in PBS supplemented with 10% fetal

calf serum and were analyzed using a FACSCanto II (BD Biosciences). For intracellular staining, single-cell suspensions were fixed and permeabilized using a ready-mixed kit from eBioscience. Fluorescence associated with nonspecific binding was subtracted using subtype-specific isotype controls. All data were evaluated with FlowJo software (Treestar).

### Histology and immunohistochemistry

For regular histology, specimens were fixed in formalin before embedding in paraffin blocks. Tissue sections were stained with hematoxylin and eosin. Images were obtained using light microscopy. For immunohistochemistry, tissue was deep-frozen in liquid nitrogen, and cryosections of 5  $\mu$ m were prepared and fixed with ice-cold acetone. Sections were rehydrated with PBS, and blocking was performed using 10% goat serum in PBS. For fluorescent labeling, unconjugated anti-B220 (RA3-6B2; BioLegend) primary antibody followed by anti-rat immunoglobulin (Ig) G Cy3-conjugated antibody (112-165-1430; Jackson ImmunoResearch) and 4,6-diamidino-2-phenylindole (Biotium) for counterstaining were used. Pictures were taken with a standard fluorescent microscope and processed with Adobe Photoshop to adjust size.

### Cell purification and adhesion assay

B cells from different secondary lymphoid organs were enriched using a magnetic-activated cell sorting CD19<sup>+</sup> B-cell isolation kit according to the manufacturer's protocol (Miltenyi Biotec). Purity of magnetically sorted B cells was >95%. Ninety-six-well plates were coated with recombinant mouse MAdCAM-Fc chimera (10  $\mu$ g/mL; R&D Systems) overnight at 4°C. The supernatant was then discarded, and wells blocked with 1% bovine serum albumin in PBS for 3 hours at room temperature. Purified B cells were cultured in RPMI 1640 medium supplemented with 10% fetal calf serum, 2 mM L-glutamine, 100  $\mu$ g/mL streptomycin, and 1 IU/mL penicillin (complete RPMI) in the presence of recombinant IFN- $\alpha$  ( $1 \times 10^3$  U/mL). B cells were labeled with carboxyfluorescein diacetate succinimidyl ester (Invitrogen) according to the manufacturer's protocol. Cells ( $10^7$ /mL in Dulbecco's modified Eagle medium without phenol red supplemented with 25 mM N-2-hydroxyethylpiperazine-N'-2-ethanesulfonic acid) were preincubated in polypropylene tubes with or without DATK32, MEL-14, or M17/4 antibody (10  $\mu$ g/mL; all from BioLegend) for 25 minutes at 37°C before cells were added to coated plates and incubated for 35 minutes at 37°C and 5% CO<sub>2</sub>. Nonadherent cells were removed by 2 to 3 washing steps with PBS. Fluorescent emission of adhesive cells was measured with a plate reader.

### In vivo homing experiments

Splenic B cells were cultured in complete RPMI with or without added IFN- $\alpha$  ( $1 \times 10^3$  U/mL) for 24 hours. Subsequently, the cell cultures were stained with carboxyfluorescein diacetate succinimidyl ester or Cell Tracker violet (both 5  $\mu$ M; Molecular Probes) according to the manufacturer's protocol. Cells ( $1 \times 10^7$ ) from each preparation were mixed and injected intravenously into naïve recipient mice. An aliquot was saved to assess the input ratio. Six hours after the adoptive transfer, cell preparations from different recipient tissues were analyzed for adoptively transferred B cells by flow cytometry. The homing index (HI) was calculated as the ratio of [IFN- $\alpha$  B cells]<sub>issue</sub> / [untreated B cells]<sub>issue</sub> / [IFN- $\alpha$  B cells]<sub>input</sub> / [untreated B cells]<sub>input</sub> as described previously.<sup>15</sup>

### Serum IgA levels

For the analysis of total serum IgG and IgA levels, 96-well plates (Nunc) were coated with goat anti-mouse IgA or goat anti-mouse IgG (Southern Biotech). For detection, peroxidase-linked anti-mouse  $\alpha$ -chain or  $\gamma$ -chain specific secondary antibody (Sigma-Aldrich) and tetramethylbenzidine substrate kit (BD Bioscience) were used.

### Statistics

All data are presented as mean  $\pm$  standard error of the mean (SEM). Statistical significance of single experimental findings was assessed with the independent 2-tailed Student *t* test. For multiple statistical comparison of a data set, the

one-way analysis of variance test with Bonferroni posttest was used. Significance was set at  $P < .05$ ,  $P < .01$ , and  $P < .001$  and was then indicated with an asterisk (\*, \*\*, and \*\*\*). All statistical calculations were performed using GraphPad Prism (GraphPad Software).

## Results

### Virus-associated immune activation causes rapid disruption of Peyer's patches

To examine the effect of virus infection on the distribution of lymphocytes in intestinal lymphoid organs, we injected mice intraperitoneally with the negative strand RNA virus VSV. This model is characterized by rapid viral spread to multiple body compartments and high systemic levels of type I IFN induction.<sup>16</sup> On inspection of the small intestine, the Peyer's patches of VSV-infected mice showed pronounced reduction in organ size that was due to a loss in cellularity (Figure 1A). A similar disruption was observed when mice were treated with poly(I:C), a synthetic double-stranded RNA analog. Poly(I:C) mimics a viral molecular pattern and stimulates the innate immune system through the activation of the Toll-like receptor 3 and the family of retinoic acid inducible gene I-like helicases.<sup>2,3</sup> Adult mice were injected twice intraperitoneally with poly(I:C) at a 3-day interval, and organs were examined 48 hours after the second injection. The total number of Peyer's patches was markedly reduced in poly(I:C)-treated mice, and the remaining Peyer's patches were barely visible macroscopically. On average, <2 Peyer's patches were identified in poly(I:C)-treated vs 8 or more Peyer's patches in untreated mice (Figure 1B). The cell numbers in Peyer's patches dropped by more than 70%. In contrast, in mesenteric lymph nodes or skin-draining PLNs cellularity remained unchanged after poly(I:C) treatment (Figure 1C). Morphologically, the Peyer's patches are formed by aggregated lymphoid follicles surrounded by the corona or subepithelial dome.<sup>17</sup> To assess changes in Peyer's patch microanatomy, organs from poly(I:C)-treated mice were examined histologically. The sections showed striking changes in the Peyer's patch architecture: Lymphoid follicles were barely visible, and the width of the subendothelial dome was markedly reduced (Figure 1D). This effect was independent of the injection route of poly(I:C) as the disruption of the Peyer's patches did not differ when poly(I:C) was applied intravenously instead of intraperitoneally (supplemental Figure 1).

In the remaining Peyer's patches, the poly(I:C)-induced loss of cellularity affected all lymphocyte subsets (Figure 2A). However, the effect was most prominent among B cells, which form the most abundant lymphocyte population in these lymphoid organs.<sup>17</sup> Indeed, the overall frequency of B cells within the Peyer's patches dropped by  $37 \pm 14\%$ , whereas other cell types showed constant frequencies (Figure 2B). In contrast, in PLNs the absolute number and frequency of B cells were increased following poly(I:C) treatment (Figure 2C-D). Because the observed loss of cellularity was mainly due to decreased B-cell numbers, we focused our following work on this subset.

### Disruption of the Peyer's patches is dependent on type I IFNs

In the mammalian antiviral immune response, the release of type I IFN plays a central role. Activation of pattern-recognition receptors by poly(I:C) leads to the production of a large amount of the type I IFNs IFN- $\alpha$  and IFN- $\beta$ , which both signal through the IFN- $\alpha$  receptor.<sup>18</sup> To investigate the role of type I IFN in poly(I:C)-induced disruption of the Peyer's patches, we treated IFNAR<sup>-/-</sup> mice with

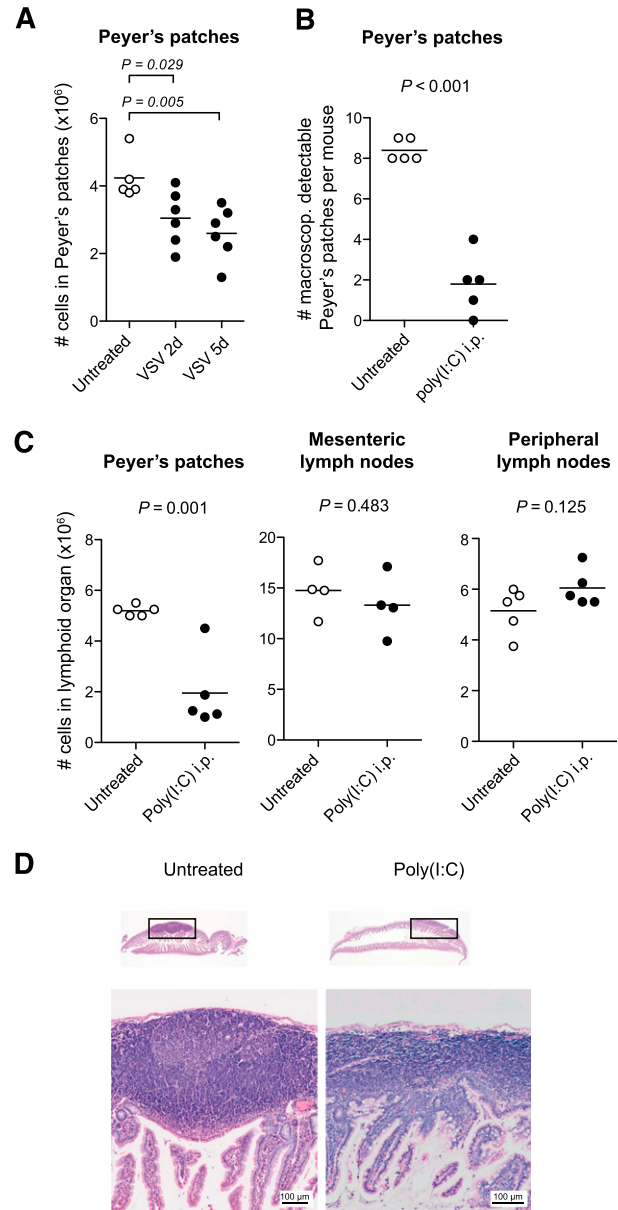


**Figure 1. Virus-associated immune activation causes rapid disruption of Peyer's patches.** (A) Mice were infected with VSV, and 2 or 5 days later, all macroscopically detectable Peyer's patches were isolated. The total cell count for all Peyer's patches per mouse was determined. (B-D) Mice were treated twice (days 0 and 3) with poly(I:C), and organs were examined 48 hours after the second injection. (B) Number of macroscopically detectable Peyer's patches per mouse. (C) Mean number of cells in lymphoid compartments per mouse. (A-C) Each data point represents 1 individual mouse, and the mean of at least  $n = 4$  mice per group is depicted as a bar. All data are representative of at least 2 independent experiments. (D) Hematoxylin and eosin-stained paraffin sections of the small intestine from 1 untreated and 1 poly(I:C)-treated mouse. The boxes indicate the Peyer's patches depicted below with  $\times 40$  magnification. These sections are representative of  $n = 3$  mice per group. i.p., intraperitoneally.

poly(I:C). In contrast to the reduced cellularity in Peyer's patches of wild-type mice, IFNAR<sup>-/-</sup> mice showed no change in cell numbers in these organs following poly(I:C) treatment (Figure 3A). Furthermore, treatment of mice with recombinant IFN- $\alpha$  also led to the disruption of Peyer's patches, demonstrating a direct involvement of type I IFN (Figure 3B). Two essential mechanisms by which type I IFN can prevent viral replication are the induction of apoptosis<sup>19</sup> and the suppression of proliferation in host cells.<sup>20</sup> To investigate

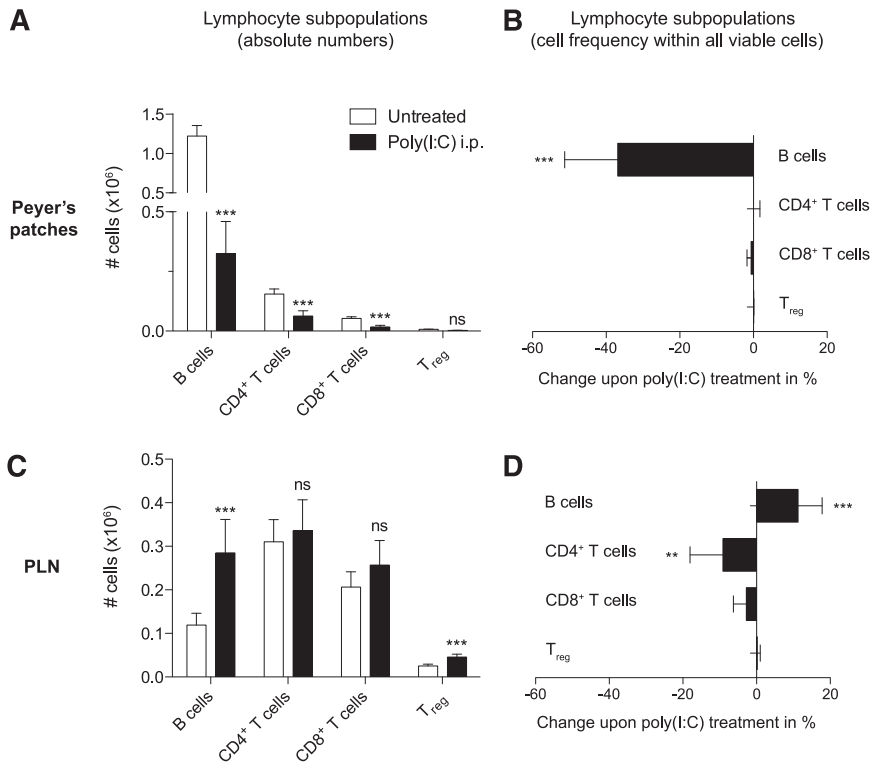


**Figure 2. Disruption of Peyer's patches is due to a decrease in B-cell numbers.** Mice were treated with poly(I:C) as in Figure 1. Lymphocyte subpopulations were analyzed by flow cytometry. Absolute cell numbers of lymphocyte subpopulations (A,C) and poly(I:C)-induced change of lymphocyte subpopulation frequency within all viable cells (B,D) (difference from untreated in %) in Peyer's patches and PLNs were determined. Data indicate the mean value of  $n = 5$  mice  $\pm$  SEM and are representative of at least 3 independent experiments. T<sub>reg</sub>, regulatory T cells.

whether these mechanisms were involved in the disruption of Peyer's patches, we first quantified B-cell proliferation by measuring their *in vivo* incorporation of 5-bromo-2'-deoxyuridine. Following poly(I:C) treatment, we observed an increased B-cell proliferation in the spleen but no changes within Peyer's patches or PLNs (supplemental Figure 2A). To evaluate the role of apoptosis in the disruption of Peyer's patches, we determined the percentage of apoptotic B cells within lymphoid organs upon treatment with poly(I:C). Surprisingly, early apoptotic B cells were slightly reduced in both PLNs and Peyer's patches, whereas there was little increase in late apoptotic B cells in Peyer's patches (supplemental Figure 2B). Taken together, these data show that the disruption of the Peyer's patches following poly(I:C) treatment is dependent on type I IFN but cannot be explained by changes in B-cell proliferation or apoptosis.

**Treatment of mice with the S1P<sub>1</sub>-blocking agent FTY720 counteracts immune-induced disruption of the Peyer's patches**

Previous reports have demonstrated that the S1P<sub>1</sub> is essential for lymphocyte recirculation and that it regulates egress from both thymus and peripheral lymphoid organs.<sup>21</sup> Following poly(I:C) treatment, type I IFN has been shown to induce lymphocyte expression of CD69, which forms a complex with and thus negatively regulates S1P<sub>1</sub>, resulting in reduced T- and B-cell egress from PLNs and their accumulation in these lymph nodes.<sup>7</sup> Based on our novel findings that organ cellularity increases in PLNs but decreases in Peyer's patches following innate immune activation, we hypothesized that S1P<sub>1</sub>-dependent B-cell egress from these tissues might be regulated in opposite ways. Thus, the poly(I:C)-induced disruption of Peyer's patches could be caused by an enhanced B-cell egress from these

**Figure 3. Disruption of the Peyer's patches is dependent on type I IFNs.** (A) Mice were treated as in Figure 1, and organs were examined 48 hours after the last poly(I:C) injection. Cell numbers in Peyer's patches and PLNs of wild-type and IFN $\alpha$ R<sup>-/-</sup> mice are shown. Each data point represents 1 individual mouse, and the mean of  $n = 5$  mice per group is depicted as a bar. (B) Mice were treated with recombinant IFN- $\alpha$ , and organs were examined 24 hours after the last injection. Cell numbers in Peyer's patches are shown. Each data point represents 1 individual mouse, and the mean of  $n = 6$  mice per group is depicted as a bar. Data are representative of 2 independent experiments.

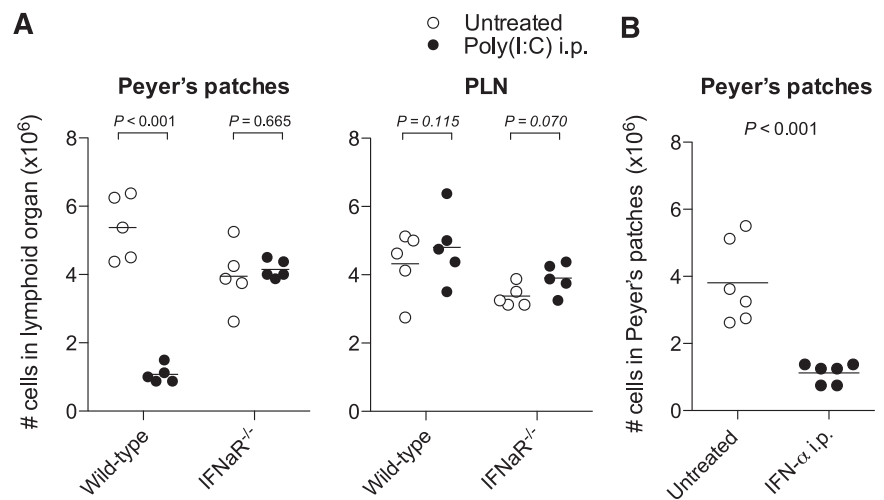
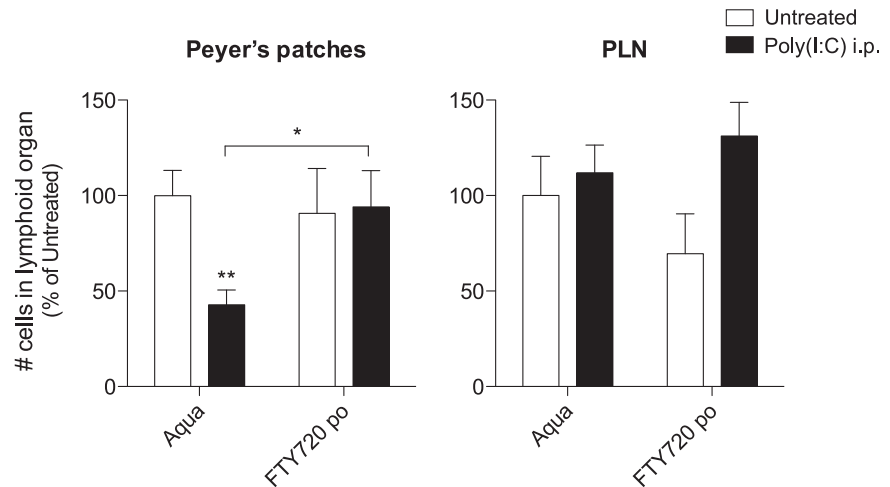


**Figure 4. Treatment of mice with the S1P<sub>1</sub>-blocking agent FTY720 counteracts immune-induced disruption of the Peyer's patches.** Mice were provided with drinking water supplemented with FTY720 and treated with poly(I:C) as in Figure 1. Organs were examined 48 hours after the last poly(I:C) injection for absolute cell numbers. Data give the mean values of n = 10 mice per group ± SEM from 2 independent experiments.



organs. To investigate whether B-cell efflux from Peyer's patches is increased during innate immune activation, mice were injected twice with poly(I:C) following pretreatment with FTY720. This immunosuppressant drug has been shown to inhibit lymphocyte emigration from lymphoid organs by downregulating S1P<sub>1</sub>.<sup>21</sup> FTY720 treatment alone did not significantly change absolute cell numbers in Peyer's patches or PLNs (Figure 4). Strikingly, mice that were pretreated with FTY720 did not show reduced cellularity of Peyer's patches following 2 injections of poly(I:C). Thus, FTY720 treatment counteracts the poly(I:C)-induced disruption of Peyer's patches. In view of the known effect of FTY720 on S1P<sub>1</sub>-mediated lymphocyte migration, we concluded that the disruption might be due to increased S1P<sub>1</sub>-dependent lymphocyte egress.

#### Stimulation with type I IFN results in reduced B-cell homing to Peyer's patches

To test this hypothesis, we compared S1P<sub>1</sub> messenger RNA levels in B cells from PLNs and Peyer's patches following poly(I:C) treatment. In line with previous reports,<sup>7</sup> S1P<sub>1</sub> transcripts were rapidly reduced in B cells from PLNs (supplemental Figure 3A). However, B cells in Peyer's patches also showed downregulated S1P<sub>1</sub> messenger RNA levels after poly(I:C) treatment. Flow cytometry analysis confirmed that B cells in both PLNs and Peyer's patches showed similarly reduced expression of S1P<sub>1</sub> after injection of poly(I:C) (supplemental Figure 3B). As described previously,<sup>21</sup> the reduced expression of S1P<sub>1</sub> on B cells from PLNs of poly(I:C)-treated mice translated into impaired B-cell ability to migrate toward an S1P<sub>1</sub> gradient in vitro (supplemental Figure 3C). B cells prepared from Peyer's patches of poly(I:C)-treated mice showed similarly reduced in vitro chemotaxis toward S1P<sub>1</sub>. Taken together, these data demonstrate that following poly(I:C) treatment, B cells in Peyer's patches do not show an increase but rather show a decrease in S1P<sub>1</sub>-dependent migration, similar to the reduced migration described for B cells in PLNs.<sup>21</sup> Hence, the striking difference in cellularity of Peyer's patches and PLNs in poly(I:C)-treated mice is unlikely to be due to opposite regulation of S1P<sub>1</sub>-dependent lymphocyte egress.

Previous reports highlighted that FTY720 not only affects S1P<sub>1</sub>-dependent egress of lymphocytes but also enhances their homing into secondary lymphoid organs.<sup>22</sup> We therefore hypothesized that poly(I:C) and type I IFN cause disruption of Peyer's patches by decreasing the entry of B cells into these organs and that this mechanism is counteracted by FTY720. Lymphocyte homing is guided by a pattern of site-specific surface molecules such as

integrins that direct them to different tissue compartments. The integrin  $\alpha_4\beta_7$  is essential for lymphocyte entry into Peyer's patches and the intestinal lamina propria through interaction with its ligand, the mucosal addressin cell adhesion molecule-1 (MAdCAM-1), which is locally expressed on specialized high endothelial venules in these tissues.<sup>23-25</sup> At the same time, lymphocytes express CD62L (L-selectin), which allows for their influx into PLNs<sup>26</sup> but also plays a role in their migration to Peyer's patches.<sup>27</sup> To investigate whether type I IFN-dependent disruption of Peyer's patches might be due to reduced B-cell entry into these lymphoid organs, we first determined the expression of the adhesion molecules  $\alpha_4\beta_7$  and CD62L on IFN- $\alpha$ -treated splenic B cells. IFN- $\alpha$ -activated B cells showed increased expression of the early activation marker CD69 and moderately increased levels of CD62L but downregulated surface expression of the gut-homing integrin  $\alpha_4\beta_7$  (Figure 5A). Consistent with these findings, IFN- $\alpha$ -stimulated B cells showed reduced in vitro binding to MAdCAM-1 (Figure 5B). This reduction was comparable to that seen with an  $\alpha_4\beta_7$ -blocking antibody. Pretreatment with antibodies that inhibit the adhesion molecules CD62L or lymphocyte function-associated antigen 1 did not influence B-cell adhesion to recombinant MAdCAM-1.

The modified expression pattern of adhesion molecules and binding characteristics of the IFN- $\alpha$ -activated B cells translated into an essentially altered in vivo homing behavior. Following adoptive transfer into naïve recipient mice, IFN- $\alpha$ -activated B cells showed reduced immigration into Peyer's patches when compared with cotransferred unstimulated cells (Figure 5C). In contrast, IFN- $\alpha$  pretreatment increased B-cell migration to PLNs. Homing to spleen was not influenced by IFN- $\alpha$  activation. Taken together, these data demonstrate that IFN- $\alpha$  downregulates expression of the gut-homing molecule  $\alpha_4\beta_7$  and selectively blocks B-cell trafficking to the Peyer's patches. Thus, we conclude that poly(I:C) and type I IFN-induced disruption of the Peyer's patches is caused by a reduced influx of B cells into the Peyer's patches. Indeed, acute blockade of  $\alpha_4\beta_7$  function in vivo following a single injection of anti- $\alpha_4\beta_7$  antibody led to rapid loss of Peyer's patch cellularity (Figure 5D), whereas cell numbers in spleen and PLNs were not significantly altered. Thus, the changes in organ cellularity induced by  $\alpha_4\beta_7$  blockade mirror the effects of poly(I:C)-mediated type I IFN release.

Previous reports have demonstrated that expression of the  $\alpha_4\beta_7$  integrin is important not only for B-cell entry into Peyer's patches but also for their trafficking to the intestinal lamina propria, this being a prerequisite for the effective clearance of an intestinal virus

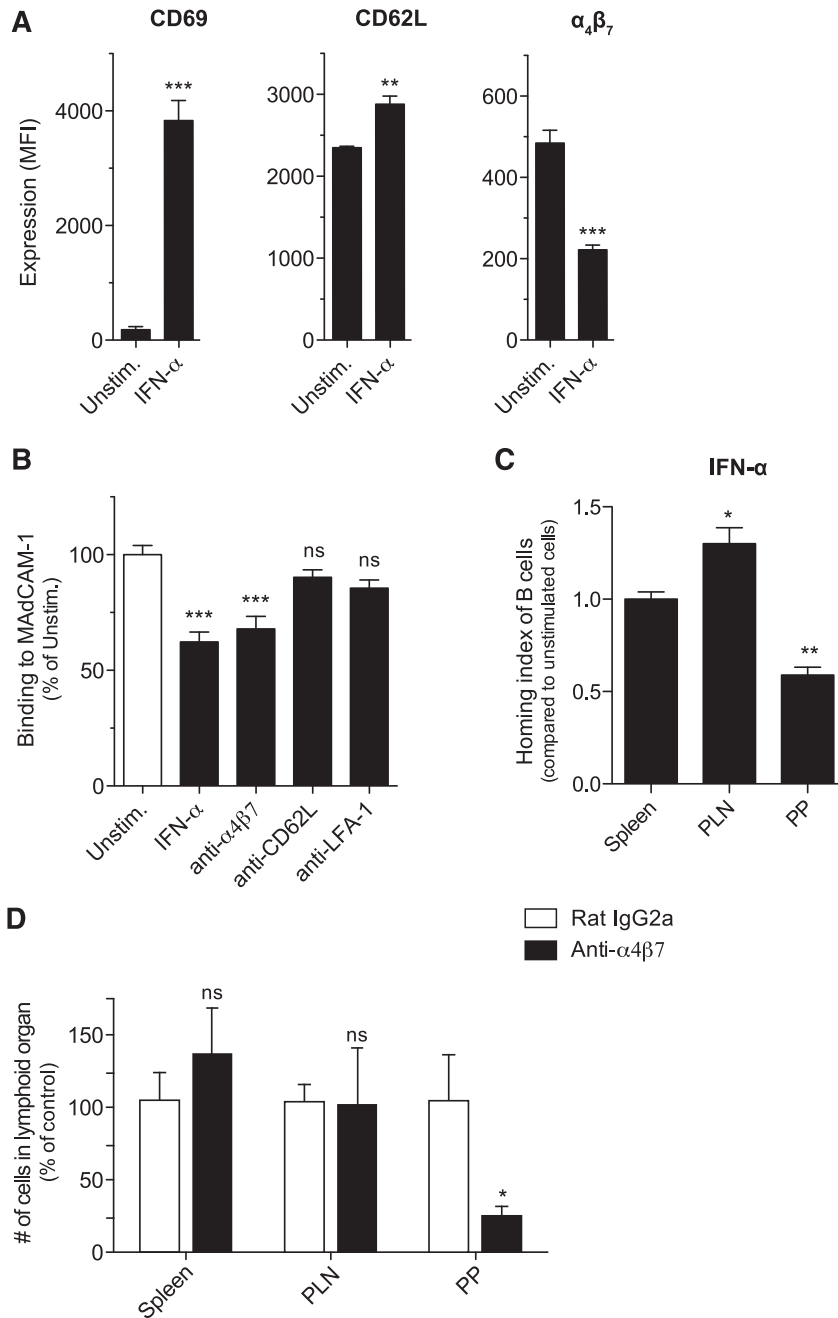


**Figure 5. Stimulation with type I IFN results in reduced B-cell homing to Peyer's patches.** Purified splenic B cells were cultured in the presence of recombinant IFN- $\alpha$  for 24 hours. (A) Surface expression of CD69, CD62L, and  $\alpha_4\beta_7$  was determined by flow cytometry. (B) Splenic B cells were either stimulated with IFN- $\alpha$  or treated with adhesion molecule–blocking antibodies. Binding of the fluorescently labeled cells to plate-bound MAAdCAM-1 was determined by spectrophotometer. All data give the mean value of triplicate samples  $\pm$  SEM. (C) IFN- $\alpha$ -stimulated splenic B cells were fluorescently labeled and adoptively transferred into naïve recipient mice. Four hours later, recipients were euthanized, and lymphoid organs assessed for the presence of transferred B cells. The HI represents the ratio of IFN- $\alpha$ -activated B cells to unstimulated B cells. Data show the mean value of individual recipient mice ( $n = 3$ )  $\pm$  SEM. The asterisk indicates comparison with the HI for the spleen. (D) Mice were injected intraperitoneally with an anti- $\alpha_4\beta_7$  or an isotype control antibody. Twenty-four hours later, cell numbers in secondary lymphoid organs were determined by flow cytometry. Data show the mean value of individual mice ( $n = 7$  for Peyer's patches and spleen,  $n = 4$  for PLNs)  $\pm$  SEM pooled from 2 independent experiments. All data are representative of at least 2 independent experiments. LFA-1, lymphocyte function-associated antigen 1; MFI, mean fluorescence intensity; PP, Peyer's patches; Unstim, unstimulated.

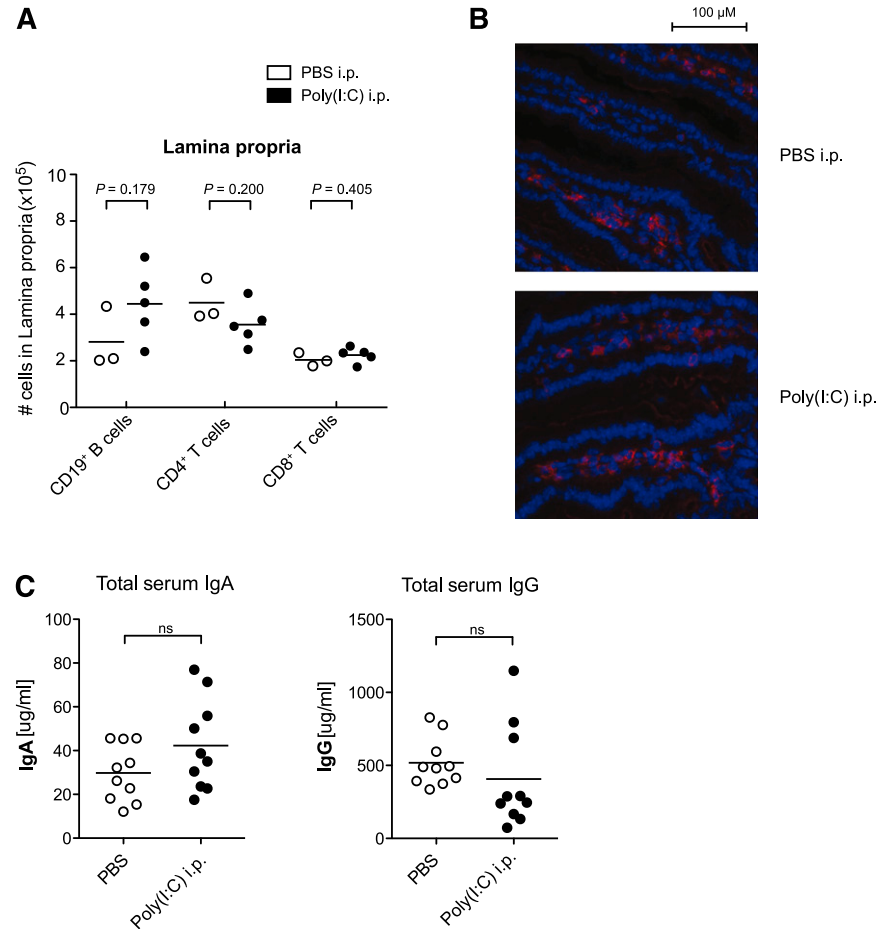
infection.<sup>28</sup> Therefore, we investigated whether downregulation of  $\alpha_4\beta_7$  following virus-associated innate immune activation has an impact on lymphocyte distribution in the intestinal lamina propria. Repetitive treatments with poly(I:C) did not influence lymphocyte numbers nor their localization within the small intestine lamina propria (Figure 6A-B). Compatibly, serum levels of IgA, which is predominantly associated with mucosal immunity, were not altered following poly(I:C) treatment (Figure 6C).

#### Disruption of the Peyer's patches is a self-limiting process

Upon viral infection or stimulation by synthetic ligands such as poly(I:C), the secretion of type I IFN is typically an early and short-lasting event.<sup>29</sup> As the Peyer's patch loss in cellularity is dependent on type I IFNs, we examined whether the effect is reversible upon termination

of IFN-inducing poly(I:C) treatment. Therefore, we examined  $\alpha_4\beta_7$  and CD69 expression following a single injection of poly(I:C) on circulating B cells, which give rise to the B-cell population of Peyer's patches. And, indeed, the downregulation of the gut-homing integrin  $\alpha_4\beta_7$  observed on B cells after poly(I:C) treatment peaked at  $\sim$ 12 hours and was restored to baseline level 96 hours postinjection (Figure 7A-B). Interestingly, this process occurred simultaneously with the upregulation of the activation marker CD69, which has been shown to bind and negatively regulate SIP1.<sup>7</sup> In line with the transient  $\alpha_4\beta_7$  downregulation, diminished cellularity of the Peyer's patches induced by 2 consecutive poly(I:C) treatments had returned to baseline levels 20 days after the last injection (Figure 7C). These data suggest that immune-induced disruption of Peyer's patches is self-limiting and that organ integrity is restored after cessation of viral innate immune activation.

**Figure 6. Virus-associated innate immune activation does not alter lymphocyte numbers in the intestinal lamina propria.** Mice were treated with poly(I:C) as in Figure 1. (A) Absolute lymphocyte numbers in the intestinal lamina propria were determined by flow cytometry. Each data point represents 1 individual mouse, and the mean of  $n = 5$  poly(I:C)-stimulated and  $n = 3$  untreated mice per group is depicted as a bar. (B) Distribution of B220<sup>+</sup> B cells (red) in the intestinal lamina propria was analyzed by immunohistochemistry. (C) Serum levels of IgA and IgG were determined by enzyme-linked immunosorbent assay. Each data point represents 1 individual mouse, and the mean of  $n = 10$  mice per group is depicted as a bar. All data are representative of at least 2 independent experiments.



## Discussion

The disruption of Peyer's patches observed in our study is reminiscent of the changes described in mice that genetically lack the adhesion molecule  $\beta_7$  integrin or its regulating transcription factor, Kruppel-like factor 2.<sup>30,31</sup> These mice are characterized by smaller numbers of Peyer's patches and reduced cellularity within these organs compared with wild-type mice. Furthermore, we show a similar phenotype after a single injection of a neutralizing antibody against  $\alpha_4\beta_7$  resulting in a rapid and strong decrease in the cellularity of Peyer's patches. In transfer experiments, we have shown that IFN- $\alpha$  stimulation selectively impairs migration of B cells to Peyer's patches, whereas recirculation to PLNs is moderately increased. This homing pattern mimics the migratory capacity of lymphocytes that either genetically lack the  $\beta_7$  subunit or have been treated with neutralizing antibodies against the  $\alpha_4\beta_7$  heterodimer or its subunits.<sup>24,30,32</sup> Indeed, we demonstrate that IFN- $\alpha$ -activated B cells downregulate the integrin heterodimer  $\alpha_4\beta_7$  and that this is associated with reduced binding to its endothelial ligand MAdCAM-1. In contrast to the impaired homing to the Peyer's patches,  $\beta_7$ -deficient lymphocytes have been described to show only little change in recirculation to mesenteric or PLNs. This is due to the redundant activity of the adhesion molecule CD62L, which can partly compensate for the absence of  $\alpha_4\beta_7$ .<sup>33</sup> Compatibly, we observed a moderately increased expression of CD62L following virus-associated innate immune activation and stable B-cell numbers in mesenteric lymph nodes and PLNs. We also observed that B-cell

distribution within the intestinal lamina propria, which is also dependent on the  $\alpha_4\beta_7$  integrin, was not altered following virus-associated innate immune activation. In general, the changes in B-cell trafficking to gut-associated lymphoid tissue following viral immune activation show parallels to the recently observed modifications in the homing of bystander-activated CD8 T cells during acute bacterial infection.<sup>34</sup>

Disruption of the Peyer's patches was prevented when mice were pretreated with the immunomodulatory compound FTY720, which was initially described to block SIP<sub>1</sub>-dependent lymphocyte egress from thymus and PLNs.<sup>21</sup> However, after poly(I:C) immune activation, we did not observe increased B-cell responsiveness to SIP<sub>1</sub> in Peyer's patches, which could have accounted for reduced organ cellularity and disruption. Thus, the prevention of Peyer's patch disruption associated with FTY720 was unlikely to stem from a blockage of B-cell egress from secondary lymphoid organs. Indeed, a later study suggested that, in addition to its effect on lymphocyte egress, FTY720 can reinforce lymphocyte interactions with high endothelial venules and thus rescue the immigration defects of  $\beta_2$ - or  $\beta_7$ -integrin single-deficient lymphocytes into secondary lymphoid organs.<sup>35</sup> Thereby, FTY720 treatment does not activate alternative homing mechanisms but rather seems to shift the balance of distinct molecular mechanisms during the extravasation process by extending the retention time of the lymphocytes on the endothelial surfaces. We suggest that the absence of Peyer's patch disruption in FTY720-pretreated mice is due to reinforced lymphocyte-endothelium interactions that compensate for reduced B-cell

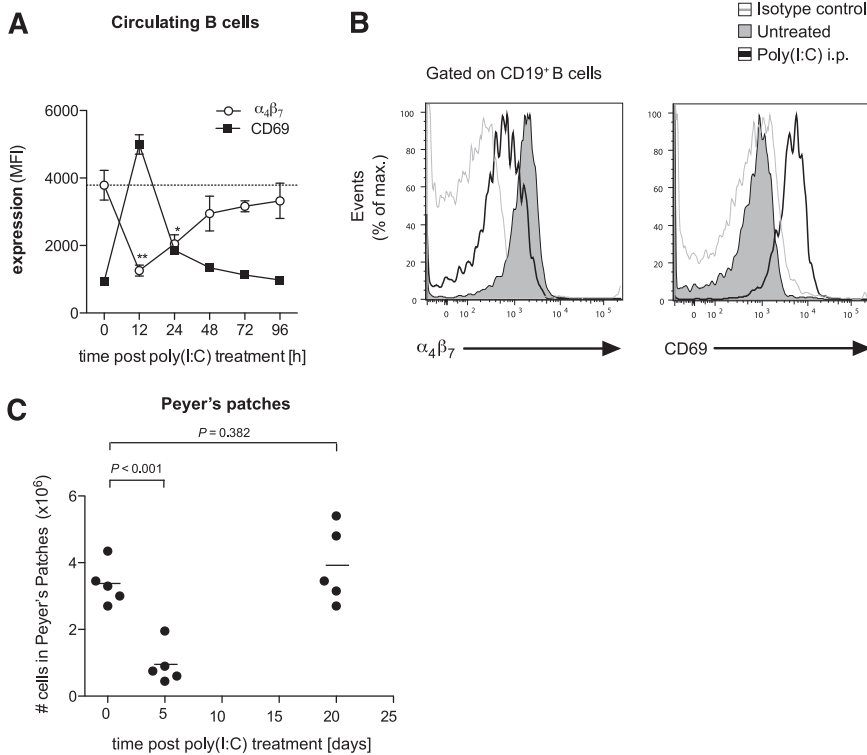


**Figure 7. Disruption of the Peyer's patches is a self-limiting process.** (A) Time course of  $\alpha_4\beta_7$  and CD69 expression on circulating B cells in the peripheral blood after a single injection of poly(I:C). Data give the mean value of  $n = 3$  individual mice  $\pm$  SEM. The dashed line represents the baseline level of  $\alpha_4\beta_7$  expression before treatment. (B) Representative histograms are gated on CD19<sup>+</sup> blood-borne B cells and give  $\alpha_4\beta_7$  and CD69 expression 12 hours after poly(I:C) treatment (thin gray line, isotype control). (C) Mice were treated with poly(I:C) as in Figure 1. Time course of total cell numbers in Peyer's patches after the last injection. Each data point represents 1 individual mouse, and the mean of  $n = 5$  mice per group is depicted as a bar. All data are representative of at least 2 independent experiments.

$\alpha_4\beta_7$  expression upon poly(I:C) injection. In line with previous reports,<sup>21</sup> we found that administration of FTY720 led to pronounced lymphopenia, which is, however, not expected to significantly impact homeostatic lymphocyte homing to the Peyer's patches.<sup>36</sup>

Interestingly, we found that reduced B-cell expression of  $\alpha_4\beta_7$  and associated disruption of Peyer's patches is self-limiting and that lymphoid organ cell numbers return to baseline levels once the systemic immune activation induced by virus-associated molecular patterns has ceased. Such transient modulation of factors that influence homeostatic trafficking and motility of lymphocytes has been suggested as a mechanism of the adaptive immune response to orchestrate local cellularity, thus limiting competition for space and resources during ongoing immune responses.<sup>37</sup> Indeed, Mueller et al<sup>37</sup> demonstrated that during viral infection certain chemokines that guide lymphocyte migration into lymphoid organs can be downregulated, thereby shaping the specificity of the newly generated memory cell pool. Our findings show 2 new aspects of this concept: (1) that not only chemokines but also integrins participate in these regulatory mechanisms; and (2) trafficking of newly activated noncognate lymphocytes can be controlled in a tissue-specific manner.

During systemic infection, the type I IFN-dependent transient rerouting of B-cell trafficking may also serve to redirect a polyclonal population of B cells to the systemic circulation where antigens are present. Indeed, systemic infection of mice with murine leukemia viruses leads to a dramatic enlargement of spleen and lymph nodes that is associated with atrophy of the Peyer's patches and a predominant B-cell loss.<sup>38</sup> Oral infection with rotavirus, a pathogen with gastrointestinal tropism, leads to hyperplasia of the Peyer's patches in mice.<sup>10,39</sup> In this model of intestinal infection, local proliferation of antigen-specific B and T cells in the Peyer's patches may block or simply mask reduction in noncognate B cells.<sup>28,40</sup> During chronic virus infections, prolonged type I IFN release has been associated with hyperimmune activation, disruption of lymphoid tissue architecture, and disease progression.<sup>41,42</sup> It is thus possible that during chronic

immune activation, prolonged changes in B-cell homing patterns may in fact hinder the control of virus replication. Generally, understanding the regulation of lymphocyte distribution during viral immune activation may open new possibilities for the treatment of associated immune pathologies. In addition, potent synthetic inducers of type I IFN such as poly(I:C) have evolved as a promising tool to modulate the immune system for therapeutic purposes.<sup>43</sup> Recombinant type I IFNs are commonly used for the treatment of cancer and chronic viral infections such as hepatitis.<sup>44,45</sup> Such therapeutic utilization of highly concentrated type I IFN could affect Peyer's patch cellularity in humans, and thus the impact on intestinal immune function should be considered, especially in the case of chronic regimens.

## Acknowledgments

The authors thank G. Ziegler (University of Munich) for help with histology sections.

This work was supported by grants from the LMUexcellent research professorship (S.E.), the German Research Foundation (DFG En 169/7-2 and Graduiertenkolleg 1202) (C.B., S.E., and S.H.), the Swiss National Science Foundation (project 138284) (C.B.), Krebsforschung Schweiz (KFS 2910-02-2012), the excellence cluster Center for Integrated Protein Science Munich 114 (S.E.), and BayImmuNet (C.B., S.K., and S.E.).

This work is part of the doctoral theses of B.B., N. Stephan, and N. Suhartha at the Ludwig-Maximilian University of Munich.

## Authorship

Contribution: S.H., D.A., and C.B. designed the research and analyzed and interpreted the results; S.H. and C.B. prepared the manuscript; S.H.,



B.B., N. Stephan, W.P.F., N. Suhartha, N. Sandholzer, and T.H. did the experiments; S.R.-S. did histology sections; K.E. performed virus infections; C.H. and S.K. gave methodologic support and conceptual advice; and C.B. and S.E. guided the study.

Conflict-of-interest disclosure: The authors declare no competing financial interests.

Correspondence: Carole Bourquin, University of Fribourg, 1700 Fribourg, Switzerland; e-mail: carole.bourquin@unifr.ch.

## References

- Kato H, Takahashi K, Fujita T. RIG-I-like receptors: cytoplasmic sensors for non-self RNA. *Immunol Rev*. 2011;243(1):91-98.
- Kato H, Takeuchi O, Sato S, et al. Differential roles of MDA5 and RIG-I helicases in the recognition of RNA viruses. *Nature*. 2006;441(7089):101-105.
- Barton GM. Viral recognition by Toll-like receptors. *Semin Immunol*. 2007;19(1):33-40.
- López CB, Hermesh T. Systemic responses during local viral infections: type I IFNs sound the alarm. *Curr Opin Immunol*. 2011;23(4):495-499.
- Essers MA, Offner S, Blanco-Bose WE, et al. IFN $\alpha$  activates dormant haematopoietic stem cells in vivo. *Nature*. 2009;458(7240):904-908.
- Anz D, Thaler R, Stephan N, et al. Activation of melanoma differentiation-associated gene 5 causes rapid involution of the thymus. *J Immunol*. 2009;182(10):6044-6050.
- Shiow LR, Rosen DB, Brdicová N, et al. CD69 acts downstream of interferon- $\alpha$ /beta to inhibit S1P1 and lymphocyte egress from lymphoid organs. *Nature*. 2006;440(7083):540-544.
- Openshaw PJ. Crossing barriers: infections of the lung and the gut. *Mucosal Immunol*. 2009;2(2):100-102.
- Narváez CF, Angel J, Franco MA. Interaction of rotavirus with human myeloid dendritic cells. *J Virol*. 2005;79(23):14526-14535.
- Lopez-Guerrero DV, Meza-Perez S, Ramirez-Pliego O, et al. Rotavirus infection activates dendritic cells from Peyer's patches in adult mice. *J Virol*. 2010;84(4):1856-1866.
- Müller U, Steinhoff U, Reis LF, et al. Functional role of type I and type II interferons in antiviral defense. *Science*. 1994;264(5167):1918-1921.
- Bourquin C, Schmidt L, Hornung V, et al. Immunostimulatory RNA oligonucleotides trigger an antigen-specific cytotoxic T-cell and IgG2a response. *Blood*. 2007;109(7):2953-2960.
- Macpherson AJ, Uhr T. Induction of protective IgA by intestinal dendritic cells carrying commensal bacteria. *Science*. 2004;303(5664):1662-1665.
- Sheridan BS, Lefrançois L. Isolation of mouse lymphocytes from small intestine tissues. In: Coligan JE, Bierer B, Margulies DH, Shevach EM, Strober W, Coico R, Brown P, Donovan JC, Kruisbeek AM, eds. *Current Protocols in Immunology*. Hoboken, NJ: John Wiley & Sons, Inc.; 2012:3.19.1-3.19.11.
- Mora JR, Bono MR, Manjunath N, et al. Selective imprinting of gut-homing T cells by Peyer's patch dendritic cells. *Nature*. 2003;424(6944):88-93.
- Trottier MD, Lyles DS, Reiss CS. Peripheral, but not central nervous system, type I interferon expression in mice in response to intranasal vesicular stomatitis virus infection. *J Neurovirol*. 2007;13(5):433-445.
- Jung C, Hugot JP, Barreau F. Peyer's patches: the immune sensors of the intestine. *Int J Inflamm*. 2010;2010:823710.
- Uzé G, Schreiber G, Piehler J, Pellegrini S. The receptor of the type I interferon family. *Curr Top Microbiol Immunol*. 2007;316:71-95.
- Clemens MJ. Interferons and apoptosis. *J Interferon Cytokine Res*. 2003;23(6):277-292.
- Petricoin EF III, Ito S, Williams BL, et al. Antiproliferative action of interferon- $\alpha$  requires components of T-cell-receptor signalling. *Nature*. 1997;390(6660):629-632.
- Matloubian M, Lo CG, Cinamon G, et al. Lymphocyte egress from thymus and peripheral lymphoid organs is dependent on S1P receptor 1. *Nature*. 2004;427(6972):355-360.
- Henning G, Ohl L, Junt T, et al. CC chemokine receptor 7-dependent and -independent pathways for lymphocyte homing: modulation by FTY720. *J Exp Med*. 2001;194(12):1875-1881.
- Bargatze RF, Jutila MA, Butcher EC. Distinct roles of L-selectin and integrins  $\alpha$ 4 $\beta$ 7 and LFA-1 in lymphocyte homing to Peyer's patch-HEV in situ: the multistep model confirmed and refined. *Immunity*. 1995;3(1):99-108.
- Wagner N, Löhler J, Kunkel EJ, et al. Critical role for  $\beta$ 7 integrins in formation of the gut-associated lymphoid tissue. *Nature*. 1996;382(6589):366-370.
- Agace WW. Tissue-tropic effector T cells: generation and targeting opportunities. *Nat Rev Immunol*. 2006;6(9):682-692.
- Arbonés ML, Ord DC, Ley K, et al. Lymphocyte homing and leukocyte rolling and migration are impaired in L-selectin-deficient mice. *Immunity*. 1994;1(4):247-260.
- von Andrian UH, Mackay CR. T-cell function and migration. Two sides of the same coin. *N Engl J Med*. 2000;343(14):1020-1034.
- Williams MB, Rosé JR, Rott LS, Franco MA, Greenberg HB, Butcher EC. The memory B cell subset responsible for the secretory IgA response and protective humoral immunity to rotavirus expresses the intestinal homing receptor,  $\alpha$ 4 $\beta$ 7. *J Immunol*. 1998;161(8):4227-4235.
- Biron CA, Cousens LP, Ruzek MC, Su HC, Salazar-Mather TP. Early cytokine responses to viral infections and their roles in shaping endogenous cellular immunity. *Adv Exp Med Biol*. 1998;452:143-149.
- Steeber DA, Tang ML, Zhang XQ, Müller W, Wagner N, Tedder TF. Efficient lymphocyte migration across high endothelial venules of mouse Peyer's patches requires overlapping expression of L-selectin and  $\beta$ 7 integrin. *J Immunol*. 1998;161(12):6638-6647.
- Winkelmann R, Sandrock L, Porstner M, et al. B cell homeostasis and plasma cell homing controlled by Krüppel-like factor 2. *Proc Natl Acad Sci USA*. 2011;108(2):710-715.
- Hamann A, Andrew DP, Jablonski-Westrich D, Holzmann B, Butcher EC. Role of  $\alpha$ 4-integrins in lymphocyte homing to mucosal tissues in vivo. *J Immunol*. 1994;152(7):3282-3293.
- Wagner N, Löhler J, Tedder TF, Rajewsky K, Müller W, Steeber DA. L-selectin and  $\beta$ 7 integrin synergistically mediate lymphocyte migration to mesenteric lymph nodes. *Eur J Immunol*. 1998;28(11):3832-3839.
- Heidegger S, Kirchner SK, Stephan N, et al. TLR activation excludes circulating naive CD8 $^{+}$  T cells from gut-associated lymphoid organs in mice. *J Immunol*. 2013;190(10):5313-5320.
- Pabst O, Herbrand H, Willenzon S, et al. Enhanced FTY720-mediated lymphocyte homing requires G $\alpha$  signaling and depends on  $\beta$ 2 and  $\beta$ 7 integrin. *J Immunol*. 2006;176(3):1474-1480.
- Pabst O, Herbrand H, Willenzon S, et al. Enhanced FTY720-mediated lymphocyte homing requires G $\alpha$  signaling and depends on  $\beta$ 2 and  $\beta$ 7 integrin. *J Immunol*. 2006;176(3):1474-1480.
- Mueller SN, Hosiawa-Meagher KA, Konieczny BT, et al. Regulation of homeostatic chemokine expression and cell trafficking during immune responses. *Science*. 2007;317(5838):670-674.
- Colombi S, Moutschen M, de Leval L, et al. Peyer's patches in murine AIDS: dissociation between lymphoproliferation and anergy. *Scand J Immunol*. 1997;45(2):175-181.
- Blutt SE, Warfield KL, Lewis DE, Conner ME. Early response to rotavirus infection involves massive B cell activation. *J Immunol*. 2002;168(11):5716-5721.
- Kuklin NA, Rott L, Feng N, et al. Protective intestinal anti-rotavirus B cell immunity is dependent on  $\alpha$ 4 $\beta$ 7 integrin expression but does not require IgA antibody production. *J Immunol*. 2001;166(3):1894-1902.
- Teijaro JR, Ng C, Lee AM, et al. Persistent LCMV infection is controlled by blockade of type I interferon signaling. *Science*. 2013;340(6129):207-211.
- Wilson EB, Yamada DH, Elsaesser H, et al. Blockade of chronic type I interferon signaling to control persistent LCMV infection. *Science*. 2013;340(6129):202-207.
- Cheng YS, Xu F. Anticancer function of polyinosinic-polycytidylic acid. *Cancer Biol Ther*. 2010;10(12):1219-1223.
- Manns MP, McHutchison JG, Gordon SC, et al. Peginterferon alfa-2b plus ribavirin compared with interferon alfa-2b plus ribavirin for initial treatment of chronic hepatitis C: a randomised trial. *Lancet*. 2001;358(9286):958-965.
- Tagliaferri P, Caraglia M, Budillon A, et al. New pharmacokinetic and pharmacodynamic tools for interferon- $\alpha$  (IFN- $\alpha$ ) treatment of human cancer. *Cancer Immunol Immunother*. 2005;54(1):1-10.